



Faculty of Electronics and Computer Engineering

**A REGION-BASED PRINCIPAL COMPONENT ANALYSIS (PCA)
TECHNIQUE FOR MEDICAL IMAGE COMPRESSION**



Lim Sin Ting

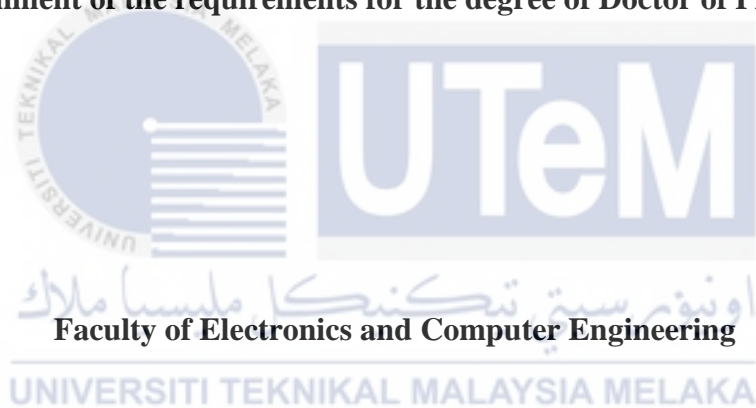
Doctor of Philosophy

2022

A REGION-BASED PRINCIPAL COMPONENT ANALYSIS (PCA) TECHNIQUE FOR MEDICAL IMAGE COMPRESSION

LIM SIN TING

**A thesis submitted
in fulfillment of the requirements for the degree of Doctor of Philosophy**



UNIVERSITI TEKNIKAL MALAYSIA MELAKA

2022

DECLARATION

I declare that this thesis entitled “A Region-based Principal Component Analysis (PCA) Technique for Medical Image Compression” is the result of my own research except as cited in the references. The thesis has not been accepted for any degree and is not concurrently submitted in candidature of any other degree.

 Signature :

Name : Lim Sin Ting

Date : 

UNIVERSITI TEKNIKAL MALAYSIA MELAKA

APPROVAL

I hereby declare that I have read this thesis and in my opinion this thesis is sufficient in terms of scope and quality for the award of Doctor of Philosophy.

Signature	:
Supervisor Name	:	Professor Dr. Nurulfajar Bin Abd Manap
Date	:



اونيورسيتي تيكنيكل مليسيا ملاك
UNIVERSITI TEKNIKAL MALAYSIA MELAKA

DEDICATION

To my beloved mother and father



ABSTRACT

Principal Component Analysis (PCA) is capable of completely decorrelating input data in the transform domain. However, PCA is limited in image compression because there is a need to encode the eigenvectors of the input data and thereby affects the rate-distortion performance. In an effort to improve rate-distortion performance, this work proposed a block-to-row PCA (BTRPCA) algorithm that employs the eigenvectors from the model image of the same image modality coupled with a row vectorization approach. Region-based compression schemes that reduce storage space while preserving the image quality of the region of interest (ROI) are receiving attention due to the increase in medical imaging data. While PCA is inherently limited by its matrix form, the Arbitrary ROI coding (ARC) proposed in this work models the ROI by means of a factorization approach and the arbitrary-shaped ROI contours and NROI are compressed using BTRPCA. In order to minimize user interaction, an automated brain segmentation technique based on midsagittal plane (MSP) and Absolute Difference Map (ADM) is then incorporated into the proposed Automated Arbitrary PCA (AAPCA). The presented result showed that BTRPCA achieves PSNR improvements of up to 10 dB compared to its PCA counterparts. The ARC outperforms JPEG, Embedded Zerotree Wavelet (EZW) and Embedded Block Coding With Optimized Truncation (EBCOT) at all tested bit rates with an average PSNR improvements of 6 dB, 18 dB and 12 dB respectively. Subjective performance analysis was in agreement with the objective performance analysis in which the AAPCA is capable of extending beyond the compression limits of the conventional PCA algorithm and that the quality of the surroundings of ROI is degrading gracefully at *bpp* as low as 0.25. The research has successfully developed an improved region-based compression scheme for medical images where lossy and lossless compression is implemented in one PCA architecture. Continuation of this study include using different encoding schemes to boost the rate-distortion performance and extraction of multiple ROI.

TEKNIK ANALISIS KOMPONEN PRINSIPAL BERASASKAN RANTAU UNTUK PEMAMPATAN IMEJ PERUBATAN

ABSTRAK

Analisis Komponen Prinsipal (PCA) berkemampuan untuk menyahsekaitan sepenuhnya data masukan di dalam domain jelmaan. Walau bagaimanapun, PCA adalah terhad di dalam pemampatan imej kerana terdapatnya keperluan untuk mengekod vektor eigen bagi data masukan dan oleh itu menjejaskan prestasi kadar herotan. Di dalam usaha meningkatkan prestasi kadar herotan, tugas ini mencadangkan algoritma PCA blok-ke-baris (BTRPCA) yang menggunakan vektor eigen daripada imej model yang terdiri dari imej modaliti yang sama yang dipadankan dengan pendekatan penvektoran baris. Skim pemampatan berasaskan rantau yang mampu mengurangkan ruangan simpanan di samping mengekalkan kualiti imej pada rantau yang diminati (ROI) menerima perhatian kerana terdapat peningkatan data di dalam data pengimejan perubatan. Walaupun PCA sememangnya terhad di dalam bentuk matriksnya, Pengekoden ROI Arbitrari (ARC) yang dicadangkan di dalam tugas ini memodelkan ROI melalui pendekatan pemfaktoran dan kontur ROI serta NROI berbentuk arbitrari yang dimampatkan menggunakan BTRPCA. Untuk meminimumkan interaksi pengguna, satu teknik pembahagian otak berdasarkan Satah Midsagittal (MSP) dan Peta Bezaan Mutlak (ADM) digabungkan di dalam PCA Arbitrari Automatik (AAPCA) yang dicadangkan. Keputusan yang dibentangkan menunjukkan bahawa BTRPCA mencapai peningkatan PSNR sehingga 10 dB berbanding rakan PCA yang lain. ARC mengatasi prestasi JPEG, Wavelet Pokok-Sifar Terbenam (EZW) dan Pengekod Blok Terbenam dengan Pemampatan Optimum (EBCOT) pada semua kadar bit yang diuji dengan purata peningkatan PSNR sebanyak 6 dB, 18 dB dan 12 dB. Analisis prestasi subjektif bersepat dengan analisis prestasi objektif, iaitu AAPCA berkemampuan untuk melangkaui had mampatan algoritma PCA konvensional dan kualiti persekitaran ROI adalah merosot dengan baik pada bpp serendah 0.25. Penyelidikan ini telah berjaya membangunkan skim pemampatan berasaskan rantau yang ditingkatkan untuk imej perubatan, di mana pemampatan hilang dan tanpa hilang dilaksanakan di dalam satu senibina PCA. Kesenambungan kajian ini termasuklah menggunakan skim pengekodan yang berbeza untuk meningkatkan prestasi kadar herotan dan pengestrakan ROI berbilang.

ACKNOWLEDGMENTS

First and foremost, I would like to express my utmost gratitude to my previous supervisor, the late Dr. David Yap Fook Weng for his expertise, enthusiasm and continuous support during the early time of this research. I am bountifully grateful to my current supervisor Associate Professor Dr. Nurulfajar Abd Manap for his invaluable advice, patience, trust, and motivation throughout the years. Thanks for the suggestions and ideas given to make this dissertation a fruitful one.

My deep appreciation also goes to the medical experts (Dr. Haba Abdullah and Mr. Daniel Chan Siang Cheng). This thesis dissertation would not have been possible without their assistance, review and time spent in the study. I will also like to express my gratitude to the student participant who helped to provide ground truth for the ROI segmentation. I am also thankful to Dr. Yeo Boon Chin, academic staff in Faculty of Engineering of Technology in Multimedia University, for providing necessary help in executing JJ2000 software. I am also thankful to the late Dr. Alan Tan Wee Chiat for sharing his expertise input on brain segmentation methods.

Last but not least, I would like to dedicate my thesis to my family members: My husband, Jia Ye for his boundless love and understanding; my loving parents, who are my beacon of lights; my brother, Dr. Lim Sin How who has been a role model for me; my elder sister Dr. Lim Sin Liang who guided me throughout my doctorate study and my younger sister Sin Qi who provides motivational support in the journey.

TABLE OF CONTENTS

	PAGE
DECLARATION	
APPROVAL	
DEDICATION	
ABSTRACT	i
ABSTRAK	ii
ACKNOWLEDGMENTS	iii
TABLE OF CONTENTS	iv
LIST OF TABLES	vii
LIST OF FIGURES	x
LIST OF APPENDICES	xxi
LIST OF ABBREVIATION	xxii
LIST OF SYMBOLS	xxiii
LIST OF PUBLICATIONS	xxiv
CHAPTER	1
1. INTRODUCTION	1
1.1 Background	1
1.2 Problem Statements	4
1.3 Research Objectives	8
1.4 Scope of Work	9
1.5 Contribution of the Thesis	10
1.6 Review of Thesis Organization	11
2. LITERATURE REVIEW	15
2.1 Medical Imaging	15
2.1.1 Introduction to MRI	16
2.1.2 MRI Brain Imaging	17
2.1.2.1 Brain Symmetry	18
2.1.2.2 T ₁ - and T ₂ -Weighted Images	19
2.2 Image Compression	20
2.2.1 Lossless Compression Techniques	21
2.2.1.1 Huffman Coding	21
2.2.1.2 Run-Length Encoding (RLE)	24
2.2.1.3 Lempel-Ziv-Welch (LZW)	24
2.2.1.4 Arithmetic Coding	24
2.2.2 Lossy Compression Techniques	21
2.2.2.1 Principal Component Analysis (PCA)	28
2.2.2.2 JPEG	28
2.2.2.3 JPEG2000	29
2.2.2.4 Embedded Zerotree Wavelet (EZW)	30
2.2.2.5 Set Partitioning In Hierarchical Tree (SPIHT)	31
2.2.3 Pros and Cons of the Techniques	33
2.3 Region-based Techniques for Medical Image Compression	35
2.3.1 ROI Selection Methods	44

2.3.1.1	Manual Segmentation	44
2.3.1.2	Automated Segmentation	45
2.3.1.3	Split-and-Merge	46
2.3.2	Segmentation Goals	47
2.3.3	Compression Methods	50
2.3.3.1	Regions with Different Quality Levels	51
2.3.3.2	Regions with Different Compression Methods	53
2.3.4	ROI Coding	56
2.3.4.1	General Scaling Based Method (GSM)	57
2.3.4.2	MAXSHIFT	57
2.3.4.3	Embedded Block Coding with Optimized Truncation	58
2.4	Introduction to Principal Component Analysis (PCA)	59
2.4.1	Data Decorrelation	59
2.4.2	The Technical Details of PCA	61
2.4.3	Image Compression Using PCA	64
2.4.3.1	Image Normalization	65
2.4.3.2	Covariance Matrix of Image Data	66
2.4.3.3	Eigenvectors and Eigenvalues of the Covariance Matrix	67
2.4.3.4	Transforming Image Data Into New Basis	68
2.4.3.5	Quantization	69
2.4.3.6	Previous Work	71
2.4.4	Block-based PCA	73
2.4.4.1	Entire Image PCA	73
2.4.4.2	Block-by-Block PCA	77
2.4.4.3	Block-to-Row Bi-Directional PCA (BTR-BD)	78
2.4.4.4	Pros and Cons of the Techniques	78
2.5	Performance Measures	79
2.5.1	Objective Measures	80
2.5.1.1	MSE (Mean Square Error)	80
2.5.1.2	PSNR (Peak Signal to Noise Ratio)	81
2.5.1.3	CoC (Correlation of Coefficient)	81
2.5.1.4	CR (Compression Ratio)	83
2.5.1.5	<i>bpp</i> (bit per pixel)	83
2.5.1.6	Histogram Analysis	84
2.5.2	Subjective Measures	84
2.6	Conclusion	85
3.	RESEARCH METHODOLOGY	
3.1	Introduction	87
3.2	Flow Chart of the Research	88
3.3	Block-to-row PCA (BTRPCA)	91
3.3.1	Framework of BTRPCA	91
3.3.2	Performance Comparison	95
3.3.3	Image Database	96
3.4	Arbitrary ROI Coding (ARC)	97
3.4.1	Framework of ARC	98
3.4.1.1	Manual Segmentation	99
3.4.1.2	ROI Shaping	100
3.4.1.3	Factorization	101

3.4.1.4	Compression	104
3.4.1.5	Region Reformation	105
3.4.2	Performance Comparison	110
3.5	Automated Arbitrary PCA (AAPCA)	113
3.5.1	Preprocessing	114
3.5.2	Midsagittal Plane (MSP) Extraction and Tilt Correction	116
3.5.3	Absolute Difference Map (ADM)	128
3.5.4	Compression	133
3.6	Summary	135
4.	RESULTS AND DISCUSSIONS	138
4.1	Results on Block-to-Row PCA (BTRPCA)	138
4.1.1	Reconstructed Image Outputs	138
4.1.2	Performance Metrics Analysis	144
4.2	Results on Arbitrary ROI Coding (ARC)	150
4.2.1	Original Image and Reconstructed Image Outputs	152
4.2.2	Histogram Analysis	159
4.2.3	Performance Metrics Analysis	162
4.2.3.1	MSE	162
4.2.3.2	PSNR	163
4.2.3.3	CoC	167
4.2.3.4	Computation Time	167
4.3	Results on Brain Segmentation Algorithm	169
4.3.1	Preprocessing	170
4.3.2	Automated Alignment of MRI Brain Scans	176
4.3.3	Absolute Difference Map (ADM)	184
4.3.4	Performance Analysis	192
4.4	Results on Automated Arbitrary PCA (AAPCA)	193
4.4.1	Original Image and Reconstructed Image Outputs	194
4.4.2	Histogram Analysis	201
4.4.3	Performance Metrics Analysis	204
4.4.3.1	MSE	206
4.4.3.2	PSNR	207
4.4.3.3	CoC	208
4.4.4	Subject Evaluation	209
4.4.5	Results Comparison with Recent Research	214
4.5	Summary	222
5.	CONCLUSION AND FUTURE WORK	228
5.1	Conclusion	228
5.2	Suggestion for Future Work	232
	REFERENCES	235
	APPENDICES	257

LIST OF TABLES

TABLE	TITLE	PAGE
1.1	Typical Image Dimensions and Uncompressed File Sizes for Common Medical Imaging Modalities (Liu et al., 2017)	2
2.1	Huffman Encoded Values for Huffman Coding Algorithm in Figure 2.6	23
2.2	Pros and Cons of the Image Compression Techniques	34
2.3	Review of Region-Based Image Compression Techniques Applied to Medical Imaging	36
2.4	An 8×8 block of Image-Pixel Values	64
2.5	Normalized Pixel Values	65
2.6	Mean for Each Dimension (Column)	66
2.7	Covariance Matrix	67
2.8	Eigenvectors with $k = 6$	68
2.9	Compressed Data \mathbf{Y} with $k = 6$	69
2.10	Compressed Data \mathbf{Y} with $k = 3$	69
2.11	Reconstructed Data \mathbf{X} with $k = 6$	70
2.12	Reconstructed Data \mathbf{X} with $k = 3$	70
2.13	Summary of PCA Algorithms Based on Performance Analysis Used	73
2.14	Mean for Each Dimension (Column)	76
2.15	Comparison Between the Block-based PCA Algorithms	79

2.16	Mean Opinion Score (MOS) for Subjective Evaluation of Images ITU-R Recommendation BT.500-3 (2002)	85
4.1	PSNR of Proposed BTRPCA and the Comparing Algorithms Using Block Size = 32, 16 and 8 on the MRI Brain Image	145
4.2	PSNR of proposed BTRPCA and the Comparing Algorithms Using Block Size = 32, 16 and 8 on the Retinal Fundus Image	145
4.3	The Computation Time (in Seconds) of Proposed BTRPCA and the Comparing Algorithms using Block Size = 32, 16 and 8 on the MRI Brain Image	146
4.4	The Computation Time (in Seconds) of Proposed BTRPCA and the Comparing Algorithms using Block Size = 32, 16 and 8 on the Retinal Fundus Image	146
4.5	Compression Results for Different Medical Images at Block Size = 8	162
4.6	The Details of the Datasets for Evaluation	169
4.7	<i>G</i> values obtained for a Left-tilted Brain Image for Varying Angle of Rotation	176
4.8	<i>G</i> values obtained for a Right-tilted Brain Image by Varying Angle of Rotation	176
4.9	Quantitative Results Comparison for MRI Brain Datasets	192
4.10	Comparative Analysis of Proposed and Entire Image PCA Algorithms (Radiopaedic)	204
4.11	Comparative Analysis of Proposed and Entire Image PCA Algorithms (Figshare)	205
4.12	Comparative Analysis of Proposed and Entire Image PCA Algorithms (Cyprus)	205

4.13	Image Sequences for Different Compressed Image	210
4.14	Contingency Table of Scores for Both Reviewers	214
4.15	Comparison of PSNR (dB) for SV and Proposed (AAPCA)	218
4.16	Segmentation and Encoding/Decoding Time of SV and Proposed AAPCA222	



LIST OF FIGURES

FIGURE	TITLE	PAGE
1.1	Compression mode spectrum	5
1.2	Outline and original contributions of thesis. This thesis is composed of 5 chapters in total. The original contributions are distributed in Chapter 3	14
2.1	Imaging planes for MRI brain images (a) Axial (b) Coronal (c) Sagittal (Sriramakrishnan et al., 2019)	17
2.2	The plane that passes through the inter-hemispheric fissure (IF) is the midsagittal plane (MSP). Illustration adapted from Davarpanah and Liew (2018)	19
2.3	Outline MSP (visible in white line) separates the brain into left hemisphere and right hemisphere. Illustration adapted from Sriramakrishnan et al. (2019)	19
2.4	T ₁ -weighted contrast (a) CSF is associated with darker pixels, white matter is associated with lighter pixels and grey matter is associated with intermediate grey-level pixels (b) Different tissues have different T ₁ relaxation. Mag. = magnetization (Pooley, 2005)	20
2.5	T ₂ -weighted contrast (a) CSF is associated with lighter pixels, white matter is associated with darker pixels and grey matter is associated	

	with intermediate grey-level pixels (b) Different tissues have different T_2 relaxation. Mag. = magnetization (Pooley, 2005)	20
2.6	Implementation of Huffman coding algorithm with binary tree	23
2.7	Implementation of arithmetic coding	26
2.8	Basic building blocks of a lossy image compression system (Hussain et al., 2018)	26
2.9	DWT three-level decomposition of MRI brain image	30
2.10	Parent-child relationships in EZW (Radha, 2011)	31
2.11	Parent-child relationships in SPIHT	33
2.12	Illustration on two types of segmentation goals in general (a) NROI as the image background and ROI as the foreground (b) NROI as the organ of study and ROI is defined as the part underlying NROI that one might wish to retain its highest quality	47
2.13	Background can be split from the image when the organ anatomy in the image has gray-level values greater than the threshold	49
2.14	Region-based compression allows the use of different compression methods ($M1$, $M2$) at different quality levels ($Q1$, $Q2$) for different regions	51
2.15	ROI scaling operation (a) Entire Image PCA compression (b) General scaling based method (c) MAXSHIFT	58
2.16	MRI brain image and its scatter plot (a) MRI brain image (b) Scatter plot of neighboring pixel value pairs where the line of best fit is represented in dashed line	59
2.17	The original data x and y are transformed to new axes defined by the principal component line of best fit (a) Plot of the first eigenvectors	

	of the data points produces the principal component line of best fit (b)	
	Original input data is transformed into new axes based only on first	
	eigenvector	61
2.18	An image is partitioned into blocks	74
2.19	Flow chart of the block-by-block PCA (Taur and Tao, 1996)	77
2.20	The corresponding noisy images of different noise variances and	
	their respective MSE, PSNR and CoC values	82
3.1	Phase development in the research	89
3.2	Flow chart in phase 1	89
3.3	Flow chart in phase 2	90
3.4	Flow chart in phase 3	90
3.5	Block diagram of the proposed BTRPCA encoder	93
3.6	Block diagram of the proposed BTRPCA decoder	95
3.7	Block diagram of the comparative study	96
3.8	Image dataset for MRI image (a) Model image (b) Test Image	97
3.9	Image dataset for retinal fundus image (a) Model image (b) Test	
	Image	97
3.10	General framework of Arbitrary ROI Coding (ARC)	99
3.11	Flowchart for the factorization program to obtain divisors for <i>num</i>	102
3.12	Flowchart of reshaping arbitrary shape ROI from a test image	103
3.13	Zeros are padded to the boundary of the image so as image size is	
	multiple of <i>n</i>	104
3.14	Illustration on region reformation (a) Arbitrary ROI selected (red	
	shaded area) (b) Mask created to mark the position of the ROI (c)	
	Masked pixels replaced by reconstructed data (blue shaded area)	106

3.15	Flowchart of Arbitrary ROI Coding (ARC)	109
3.16	Flowchart for MAXSHIFT region-based coding (JPEG Part I, 2000)	112
3.17	The framework for the proposed AAPCA model	114
3.18	Block diagram illustrates the steps to remove the image background	115
3.19	An ideal planar system (white) versus an imaging planar system (blue) when symmetries exhibited in tilted imaging modalities	117
3.20	Brain hemisphere is modeled as elliptical shape that can be tilted to the (a) right or (b) left	121
3.21	Angle of rotation θ in xy and $x'y'$ coordinate systems	121
3.22	The general framework in MSP extraction and tilt correction algorithm	126
3.23	The proposed intermediate steps to detect the edge of the skull	126
3.24	Flowchart depicts the proposed MSP extraction and tilt correction algorithm	127
3.25	The first step in ADM algorithm is to shift out-of-center centroid (a) to the center of the image as shown in (b) where centroid of the ellipse is marked by a red cross	128
3.26	Proposed Absolute Difference Map (ADM)	129
3.27	Proposed image manipulation for both separated brain hemispheres	131
3.28	The overall framework of the proposed brain segmentation system that includes four major processing parts: Image preprocessing, MSP extraction, tilt correction and ADM algorithm	133
3.29	The Automated Arbitrary PCA (AAPCA) framework	135
4.1	The reconstructed images obtained by proposed BTRPCA and the comparing algorithms where $n = 32$, $bpp = 0.5$	139

4.2	The reconstructed images obtained by proposed BTRPCA and the comparing algorithms where $n = 8$, $bpp = 0.5$	140
4.3	The reconstructed images obtained by proposed BTRPCA and the comparing algorithms where $n = 8$, $bpp = 0.125$	141
4.4	The edges of the cerebrospinal fluid (CSF) on MRI brain image is cropped and zoom in to illustrate the distortion for image compressed using proposed BTRPCA at $n = 8$, $bpp = 0.125$	142
4.5	Top left of the MRI brain image is cropped and zoom in to illustrate the blocky effects for image compressed using block-by-block PCA at $n = 8$, $bpp = 0.125$	143
4.6	Comparison of average computation time between proposed BTRPCA and the comparing algorithms for $n = 8$ and $bpp = 0.125$ on different test images	148
4.7	Test images along with their respective model images used in this study	151
4.8	Visual compression results for MRI brain image using proposed algorithm (a) Original MRI brain image (b) ROI manually segmented (c) Split NROI (d) Image reconstructed at $bpp = 1.0$ (e) Image reconstructed at $bpp = 0.5$ (f) Image reconstructed at $bpp = 0.25$ (g) Image reconstructed at $bpp = 0.125$ (h) Image reconstructed at $bpp = 0.0625$	153
4.9	Visual compression results using proposed ARC algorithm for the medical images for the bpp from 1.0 to 0.0625	154
4.10	Visual comparison results for medical images between the proposed algorithm and the Entire Image PCA algorithm at $bpp = 0.0625$	155

4.11	Visual comparison results for reconstructed MRI test images using JPEG, JPEG2000, EZW and SPIHT for <i>bpp</i> from 1.0 to 0.0625	157
4.12	Visual comparison results for reconstructed MRI test images using region-based compression methods of EBCOT, general scaling based method (GSM) and MAXSHIFT for <i>bpp</i> from 1.0 to 0.0625	158
4.13	Histograms of the Entire Image PCA algorithm (a) Histogram of original MRI brain image (b) Histogram of reconstructed image (<i>bpp</i> = 0.0625) (c) 3D histogram of original image (d) 3D histogram of reconstructed image (<i>bpp</i> = 0.0625)	160
4.14	Histograms of the proposed ARC (a) Histogram of original MRI brain image (b) Histogram of ROI (c) Histogram of NROI (d) Histogram of reconstructed image (<i>bpp</i> = 0.0625) (e) 3D histogram of original image (f) 3D histogram of reconstructed image (<i>bpp</i> = 0.0625)	161
4.15	Graphical results for proposed ARC algorithm and Entire Image PCA algorithm in terms of <i>bpp</i> vs. MSE	163
4.16	Graphical results for proposed ARC algorithm and Entire Image PCA algorithm in terms of <i>bpp</i> vs. PSNR	164
4.17	Graphical presentation of <i>bpp</i> vs. PSNR for JPEG, JPEG2000, EZW, SPIHT, Entire Image PCA and proposed ARC algorithm	165
4.18	Comparison of results between proposed methods and the existing region-based compression algorithms	165
4.19	Graphical results for proposed ARC algorithm and Entire Image PCA algorithm in terms of <i>bpp</i> vs. CoC	167

4.20	Computation time for proposed ARC algorithm and Entire Image PCA algorithm	168
4.21	Sequence of images that go through each step for T_1 -weighted and T_2 -weighted MRI images to eliminate background	171
4.22	Results of the detection of the edges from the background-removed images in Radiopaedic database	173
4.23	Results of the detection of the edges from the background-removed images in Figshare database	174
4.24	Results of the detection of the edges from the background-removed images in Cyprus database	175
4.25	$G_{threshold}$ is found by plotting G values versus $abs(\theta)$ for varying angle of rotation for left- and right-tilted brain image	177
4.26	Visual comparison of the proposed MSP extraction algorithm in extracting the symmetric axis (green line) from (a) Radiopaedic database, (b) Figshare database, and (c) Cyprus database	178
4.27	The green detection line is slightly skewed from the MSP due to uneven skull shape	179
4.28	The results of proposed tilt correction algorithm in realigning the real brain images from Radiopaedic database (a) Input images (b) Reoriented images	180
4.29	The results of proposed tilt correction algorithm in realigning the real brain images from Figshare database (a) Input images (b) Reoriented images	180

4.30	The results of proposed tilt correction algorithm in realigning the real brain images from Cyprus database (a) Input images (b) Reoriented images	181
4.31	Noise tolerance of the proposed algorithm in extracting the MSP at varying SNR (a) Brain MRI degraded with noise level of SNR = -6.75 dB (b) Brain MRI degraded with noise level of SNR = -9.07 dB (c) Brain MRI degraded with noise level of SNR = -14.31 dB	182
4.32	Asymmetry tolerance of the proposed algorithm in extracting the MSP with synthetic 'lesion' in increasing radius from (a) to (c) and gray level of 0	183
4.33	The proposed MSP algorithm failed due to lesion that deforms the shape of the skull	183
4.34	Left and right hemisphere for correct MRI brain images are extracted based on the maximum bilateral symmetry represented by MSP	184
4.35	A series of ADM operations to obtain the LCC as the ROI	186
4.36	The LCC for both hemisphere is now shown on the same image	187
4.37	Output image is free of irrelevant regions after flood-filled operation	187
4.38	The segmented pathologic tissues or the ROI (highlighted in blue) are superimposed on the MRI brain image	188
4.39	The results of proposed segmentation algorithm in extracting the real brain images from Radiopaedic database	189
4.40	The results of proposed segmentation algorithm in extracting the real brain images from Figshare database	190
4.41	The results of proposed segmentation algorithm in extracting the real brain images from Cyprus database	191

4.42	Test images used in this part of the study	194
4.43	MRI brain images from Radiopaedic database reconstructed with the proposed algorithm at different bpp and CR (a) Original images (R1, R2, R3 and R4) (b) Extracted ROI using the proposed segmentation algorithm (c) Reconstructed images at $bpp = 1.00$ (d) Reconstructed images at $bpp = 0.25$ (e) Reconstructed images at $bpp = 0.0625$	195
4.44	MRI brain images from Figshare database reconstructed with the proposed algorithm at different bpp and CR (a) Original images (F1, F2, F3 and F4) (b) Extracted ROI using the proposed segmentation algorithm (c) Reconstructed images at $bpp = 1.00$ (d) Reconstructed images at $bpp = 0.25$ (e) Reconstructed images at $bpp = 0.0625$	196
4.45	MRI brain images from Cyprus database reconstructed with the proposed algorithm at different bpp and CR (a) Original images (C1, C2, C3 and C4) (b) Extracted ROI using the proposed segmentation algorithm (c) Reconstructed images at $bpp = 1.00$ (d) Reconstructed images at $bpp = 0.25$ (e) Reconstructed images at $bpp = 0.0625$	197
4.46	Visual comparison results for R1, F1 and C1 between the proposed algorithm and the Entire Image PCA algorithm at $bpp = 0.125$. It is observed that visual quality for the proposed algorithm is better than the Entire Image PCA algorithm	199
4.47	Visual comparison results for R1, F1 and C1 between the proposed algorithm and the Entire Image PCA algorithm at $bpp = 0.0625$. The visual quality for the proposed algorithm is excellent at the same $bpp = 0.0625$ as compared to the reconstructed image by Entire Image PCA algorithm	200

4.48	Histograms of the proposed compression algorithm for R1 (a) Histogram of original MRI brain image (b) Histogram of ROI (c) Histogram of NROI (d) Histogram of reconstructed image (e) 3D histogram of original image (f) 3D histogram of reconstructed image ($bpp = 1.0$)	202
4.49	Histograms of the proposed compression algorithm for F1 (a) Histogram of original MRI brain image (b) Histogram of ROI (c) Histogram of NROI (d) Histogram of reconstructed image (e) 3D histogram of original image (f) 3D histogram of reconstructed image ($bpp = 1.0$)	203
4.50	Image sequence versus MOS for all tested image from three datasets	211
4.51	Visual comparison of ROI segmentation on R2 image (a) ROI extracted using SV algorithm (b) Image background void of ROI using SV algorithm (c) ROI extracted using proposed method (d) Image background void of ROI using proposed method	215
4.52	Visual comparison of ROI segmentation on F3 image (a) ROI extracted using SV algorithm (b) Image background void of ROI using SV algorithm (c) ROI extracted using proposed method (d) Image background void of ROI using proposed method	216
4.53	Visual comparison of ROI segmentation on C1 image (a) ROI extracted using SV algorithm (b) Image background void of ROI using SV algorithm (c) ROI extracted using proposed method (d) Image background void of ROI using proposed method	217